NIH Public Access
Author Manuscript
Hear Res. Author manuscript; available in PMC 2012 August 1.

Published in final edited form as:
Hear Res. 2011 August ; 278(1-2): 96–105. doi:10.1016/j.heares.2011.05.004.

Micropatterned Methacrylate Polymers Direct Spiral Ganglion Neurite and Schwann Cell Growth

Joseph C. Clarke[1], **Bradley W. Tuft**[2], **John D. Clinger**[1], **Rachel Levine**[1], **Lucas Sievens Figueroa**[2], **C. Allan Guymon**[2], and **Marlan R. Hansen**[1]

[1]Department of Otolaryngology-Head and Neck Surgery, University of Iowa, Iowa City, Iowa 52242

[2]Department of Chemical and Biochemical Engineering, University of Iowa, Iowa City, Iowa 52242

Abstract

Significant advances in the functional outcomes achieved with cochlear implantation will likely require tissue-engineering approaches to improve the neural prosthesis interface. One strategy is to direct spiral ganglion neuron (SGN) axon growth in a highly organized fashion to approximate or contact stimulating electrodes. Here we assessed the ability of micropatterns induced by photopolymerization in methacrylate (MA) polymer systems to direct cultured neonatal rat SGN neurite growth and alignment of SG Schwann cells (SGSCs). SGN survival and neurite length were comparable among various polymer compositions. Remarkably, there was no significant difference in SGN survival or neurite length between laminin and non-laminin coated MA polymer substrates, suggesting high biocompatibility with SG tissue. Micropatterning with photopolymerization generated microchannels with a ridge periodicity of 50 μm and channel depths of 0.6–1.0 μm. SGN neurites grew within the grooves of the microchannels. These topographies strongly induced alignment of dissociated SGN neurites and SGSCs to parallel the pattern. By contrast, fibroblasts failed to align with the micropattern suggesting cell specific responses to topographical cues. SGN neurites extending from explants turned to parallel the pattern as they encountered the microchannels. The extent of turning was significantly correlated with angle at which the neurite initially encountered the pattern. These results indicate that SGN neurites respond to microtopographical features and that these features can be used to direct neurite growth in a highly organized fashion.

1. Introduction

Deafness typically results from irreversible cochlear hair cell (HC) death followed by degeneration of the associated afferent spiral ganglion (SG) axons and the eventual death of the spiral ganglion neurons (SGNs) themselves (Alam et al., 2007; Leake et al., 1988; Spoendlin, 1975). Electrical stimulation of SGNs by cochlear implant (CI) electrodes replaces mechanosensory transduction of sound providing hearing sensation for deaf patients. However, current CI technologies provide a limited number of independent

© 2011 Elsevier B.V. All rights reserved.

Correspondence: Marlan R. Hansen, MD, Department of Otolaryngology-Head and Neck Surgery, 2PFP, University of Iowa Hospitals and Clinics, Iowa City, Iowa, 52242, Phone: (319) 353-7151, Fax: (319) 356-4547, marlan-hansen@uiowa.edu.

Publisher's Disclaimer: This is a PDF file of an unedited manuscript that has been accepted for publication. As a service to our customers we are providing this early version of the manuscript. The manuscript will undergo copyediting, typesetting, and review of the resulting proof before it is published in its final citable form. Please note that during the production process errors may be discovered which could affect the content, and all legal disclaimers that apply to the journal pertain.

NIH-PA Author Manuscript
NIH-PA Author Manuscript
NIH-PA Author Manuscript

NIH-PA Author Manuscript

NIH-PA Author Manuscript

NIH-PA Author Manuscript

channels due to interaction of nearby channels (Rubinstein, 2004; Shannon et al., 2004). These channel interactions are due, at least in part, to the distance between the neural elements in the modiolus and the stimulating electrodes in the scala tympani. The limited number of channels contributes to the poor spatial and temporal resolution of CIs and limits performance, especially for complex sounds or in environments with competing noise (Rubinstein, 2004; Shannon et al., 2004). Given these limitations, there is lively interest in improving the neural prosthesis interface by directing SGN axon regeneration to approximate or even contact the stimulating electrodes (Brors et al., 2002; Evans et al., 2009; Miller et al., 2007; Pettingill et al., 2007; Richardson et al., 2009; Roehm et al., 2005). However, to be effective, such axonal regrowth would need to be radial, recapitulating the normal pattern of afferent innervation. If successful, such tissue engineering stands to dramatically enhance the neural prosthesis interface and increase the fidelity provided by stimulating electrodes.

Strategies to direct neurite growth have typically relied on the use of micropatterned bioactive molecules (Branch et al., 2001; Branch et al., 1998; Gustavsson et al., 2007; Miller et al., 2001; Oliva et al., 2003; Schmalenberg et al., 2005). Examples include micropatterned stripes of laminin, fibronectin, or poly-L-lysine or stripes coated with EphA1/IgG-Fc-chimera that direct neurite growth from cultured spiral ganglion explants (Brors et al., 2003; Evans et al., 2007). In these cases, neurites grew preferentially on the high concentration laminin stripes and avoided the EphA1/IgG-Fc-chimera stripes. Other studies used soluble neurotrophic or chemoattractive/repulsive factors to guide neurite growth. For instance, SGN neurites grow towards a concentration gradient of neurotrophin (Altschuler et al., 1999; Dazert et al., 1998; Wise et al., 2005; Wise et al., 2010; Wittig et al., 2005). In addition to biochemical cues, many cellular processes including growth cones respond to three-dimensional topographical features in the environment (Curtis et al., 1997; Dalby et al., 2003). Recently, patterned topographies have emerged as another method to direct cellular patterning such as axon growth (Fozdar et al.,; Johansson et al., 2006) To begin to understand how SGN neurites respond to environmental topographical features we assessed the ability of stable topographic microfeatures in methacrylate polymers to guide SGN neurite growth.

Methacrylates (MAs) were among the first successful polymer systems to serve as functional biomaterials (Ratner, 2004). Their biocompatibility was first demonstrated during the development of the intraocular lens (Apple et al., 1996; Ridley, 1951) and has since been confirmed in contact lens applications (Kapoor et al., 2009), dental resins (Pameijer et al.), cellular encapsulation (Uludag et al., 2000), and bone cements (Kenny et al., 2003). Beyond biocompatibility, MAs also provide a versatile range of chemistries that allows for the design of materials with tailored chemical and mechanical properties to suit intended biological interfaces. While various methods exist to generate these biomaterials, photopolymerization, i.e. the use of light to produce polymers, has emerged as a production platform of choice due to its mild reaction conditions and high reaction rates. Moreover, photopolymerization offers unique advantages over other polymerization techniques that include: reaction environments free of volatile organic compounds or other potentially cytotoxic species, low energy input, and spatial control of the polymerization (Lee et al., 2005). Recent studies demonstrated the versatility of this technique for biological applications. For example, a photopolymerization reaction is mild enough to coencapsulate plasmid DNA and cells in a degradable, methacrylate hydrogel. Subsequent transfection of either encapsulated or plated cells is demonstrated upon release of the plasmid DNA from the gel (Quick et al., 2003). Further, 3D tissue engineering scaffolds with a range of pore sizes and architectures are generated through a single photopolymerization step in order to determine the effect of substrate geometry and porosity on cell behavior and *in vivo* reaction (Bryant et al., 2007).

NIH-PA Author Manuscript

NIH-PA Author Manuscript

NIH-PA Author Manuscript

Interestingly, specific surface topographic features such as those that could be formed via photopolymerization influence a variety of cellular responses including alignment and growth of Schwann cells (SCs) and fibroblasts (Clark et al., 1991; Dunn et al., 1986; Hsu et al., 2005). SCs support and guide axon regeneration and regenerating SGNs closely align with SCs (Whitlon et al., 2009). Furthermore, micropatterning of biomolecules to direct SC orientation also enhances and guides dorsal root ganglion neurite growth (Song et al., 2007).

Our study focuses on the use of mixtures of two MA monomers: hexyl methacrylate (HMA) and 1,6-hexanediol dimethacrylate (HDDMA), polymerized in varied proportions. These polymers, with or without laminin coating, supported SGN survival and neurite growth in culture. Photopolymerization allowed generation of micropatterns in the polymers that directed neurite growth in SG explants and dissociated cultures. We also found that micropatterned polymers promoted alignment of spiral ganglion Schwann cells (SGSCs) but not fibroblasts. Taken together these results demonstrate the biocompatibility of MA polymers with SG tissue and the ability of micropatterned topographic features to direct SGSC alignment and SGN neurite growth.

2. Materials and Methods

2.1. Photopolymerization

Monomer mixtures of HMA and HDDMA (Aldrich) were prepared with 1 wt% of 2, 2'-dimethoxy-2-phenylacetophenone as the photoinitiator (Ciba, Tarrytown, NY). A sample volume of 20 μL was pipetted onto glass microscope slides and was covered with a 50 μm periodicity glass-chrome Ronchi rule photomask (Applied Image Inc., Rochester, NY) for patterned samples, or with a glass coverslip for unpatterned samples. Polymer samples were cured under a medium pressure mercury arc lamp (Ace Glass) for 1 to 3 minutes (Fig 1). Following polymerization the samples were rinsed copiously with 95% ethanol to remove residual monomer and allowed to air dry before use.

2.2 Dissection of spiral ganglia

The institutional animal care and use committee at the University of Iowa approved all protocols used in this study. Spiral ganglia (SG) were isolated from postnatal day 4–5 (P4–P5) rats euthanized under cold anesthesia after placing the pups in a cardboard box on ice for 20 min (Danneman et al., 1997; Phifer et al., 1986). The temporal bone was harvested and the otic capsule was dissected under operating microscope in ice cold PBS. The bony cochlear capsule was removed, followed by the spiral ligament. The organ of Corti was removed, transecting the outer radial fibers, leaving the SGNs within the modiolus. Modiolar bone and surrounding connective tissue were removed. Ganglia were collected in ice cold Hanks' balanced salt solution with calcium and magnesium (HBSS+/+, Gibco, Carlsbad, CA). When used as explants, SGs were cut into 4 pieces and placed onto the prepared culture slides.

2.3. Characterization of micropatterns

Polymer topography was characterized with a Wyko NT 1100 optical profiling system (Veeco, Plainview, NY) with 20X and 50X objectives (Fig 3). Nine channel amplitude measurements were taken at random locations for each sample, and the average value was reported as the general amplitude of the substrate.

2.4. Spiral ganglion cultures

Dissociated SG cultures from P3-5 rat pups, prepared as previously described (Hansen et al., 2001a; Hansen et al., 2001b; Hegarty et al., 1997) were plated in 8 mm cloning cylinders placed on polymer surfaces with sterile silicon grease to seal the edges. Cultures were grown

NIH-PA Author Manuscript

NIH-PA Author Manuscript

NIH-PA Author Manuscript

on unpatterned polymers both with and without laminin (20 μg/mL) coating. Laminin coated glass slides were used as a control. Cultures were maintained in Dulbecco's Modified Eagle Medium (DMEM) supplemented with N2 additives and 5% fetal bovine serum. Neurotrophin-3 (NT-3) (50 ng/ml) and Brain Derived Neurotrophic Factor (BDNF) (50 ng/ml) were included in medium to promote SGN survival and neurite growth (Hansen et al., 2001a; Hegarty et al., 1997; Roehm et al., 2008). After 72 h, the cultures were fixed with 4% paraformaldehyde and stained with anti-S100 and anti-neurofilament 200 (NF200) antibodies (1:400, Sigma-Aldrich, St. Louis, MO) to label SGSCs and SGNs, respectively (Hansen et al., 2001a), followed by Alexa 488 and Alexa 546 conjugated secondary antibodies. Hoechst 3342 (10 μg/ml) was used for nuclear staining. Digital epifluorescent images were captured on a Leica DMIRE2 microscope (Leica Microsystems, Bannock, IL) with Leica DFC350FX digital camera and Metamorph software (Molecular Devices, Silicon Valley, CA). SGN cell survival was determined as before by counting the total number of viable SGNs per cloning cylinder (Hansen et al., 2001b). Only NF200-positive SGNs with non-pyknotic nuclei were considered viable. Neurite length was calculated from digital images of epifluorescence staining by measuring the longest process of 30 randomly selected SGNs per well using the measurement tool in Image J (NIH, Bethesda, MD). SG explants, prepared by cutting each ganglion into 4 segments, were grown in similar conditions and fixed after 3–4 days of growth for staining and analysis.

2.5. Determination of neurite alignment to pattern *in vitro*

To determine the alignment of neurites to micropatterns in dissociated SG cultures, neurite length was measured in Image J as previously described (Roehm, 2008). This measurement was then compared to the distance from the cell body to the nerve terminus in a straight line along the micropattern (Fig. 4A). The neurite length divided by the end-to-end distance along the polymer was calculated to represent the aligment to the pattern. A number closer to unity (1) represents a neurite that closely follows the pattern. A wandering neurite, not aligned to the pattern, would have a higher ratio of neurite length to end-to-end distance. In order to analyze neurite alignment on unpatterned polymer substrates, neurite length was compared to end-to-end distance along the horizontal plane (Fig. 4).

To determine the extent that micropatterns influenced neurite turning in explants, the angle of the neurite relative to the pattern was measured when the neurite first encountered the pattern (initial angle) and compared to the angle of the neurite terminus relative to the pattern (terminal angle). The difference between the initial and terminal angle of the neurite ($\Delta\theta$) was calculated to quantify the extent of turning induced by the micropattern (Fig. 8A). In some cases, the initial portion of individual neurites remained in bundles as they exited the explant and was not resolvable by epifluorescent microscopy. In each case, the neurites within the bundle traveled in the same trajectory and the angle of the bundle was measured to determine initial angle of the neurites comprising it.

2.6. Spiral ganglion Schwann cell and fibroblast cultures

To determine the influence of the micropatterns on fibroblasts and SC alignment in the absence of neurites, dissociated SG cultures lacking neurons were prepared as previously described (Hansen et al., 2001a). Briefly, spiral ganglia from P3-5 rat pups were enzymatically and mechanically dissociated and plated onto patterned or unpatterned HMA/HDDMA polymers in DMEM/N2 media lacking neurotrophic factors with 5% FCS to support the fibroblasts. After 2 days, the cultures were fixed and immunostained with anti-S100 antibodies. Cell orientation was determined by drawing the outline of the cell using Image J software and fitting an ellipse to the cell outline. The angle of the long axis of the ellipse relative to the pattern (θ) was then measured in Image J.

NIH-PA Author Manuscript

NIH-PA Author Manuscript

NIH-PA Author Manuscript

2.7. Statistical analyses

For statistical analysis of SGN survival and SG neurite growth a one-way ANOVA was performed with post hoc Tukey test using SigmaStat software (Systat Software, Chicago, IL). A two-tailed t-test was used to compare neurite alignment on unpatterned vs patterned polymers. To compare SGSC, fibroblast alignment on patterned and unpatterned polymers, a one way ANOVA with post-hoc Dunn's test was used.

3. Results

3.1. Methacrylate polymers support SGN survival and neurite growth *in vitro*

Varying the relative proportion of HMA and HDDMA monomer determines the cross-link density and polarity of the polymer. These properties are known to influence cell-material interactions (Bryant et al., 2004; Kim et al., 2007). Thus, we first assessed the ability of varied proportions of HMA and HDDMA polymer without micropatterns to support SGN survival and neurite growth. Polymer composition ranged from 20% to 80% HMA with the remaining percentage composed of HDDMA. A subset of polymers were coated with laminin. Equal volumes of dissociated SG cultures were grown in 8 mm cloning cylinders placed on the polymer surfaces. Control cultures were maintained on laminin-coated glass slides. After 72 hrs, the cultures were fixed and immunostained with anti-NF200 antibodies. SGN and SGSC growth was robust on all compositions of HMA/HDDMA polymers both with and without laminin coating (Fig. 2B). There was no significant difference in SGN survival between any of the individual polymer compositions and control cultures, nor between the various polymer compositions ($p=0.306$ one way ANOVA). While SGN morphology appeared similar on laminin and non-laminin coated polymers and glass, SGSCs exhibited a decrease in spindle morphology on polymers without laminin coating when compared to those grown on laminin coated polymer or glass.

Similar to neuronal survival, there was no significant difference in neurite length with variations in polymer composition ($p=0.608$ one way ANOVA) (Fig. 2C). Further, MA polymers, including those without laminin coating, supported neurite growth to the same extent as laminin-coated glass. These results confirm that MA polymers support SGN survival, neurite growth and SGSC growth. Remarkably, polymers lacking laminin coating supported SGN survival and neurite growth comparable to laminin-coated substrates.

3.2 Photopolymerization creates micropatterns in methacrylate polymers

Micropatterns were generated on sample surfaces by using the spatial control afforded by the photopolymerization process. Polymerization principally occurs in regions exposed to light irradiance and proceeds more slowly in shadowed regions. Therefore, spatial control of the reaction is achieved by directing the light to areas intended for the polymerization while blocking or reducing the amount of light absorbed at others. In this study, UV light was directed by placing a simple photomask, with 25μm wide alternating bands (periodicity of 50 μm) that either transmit or reflect light, between the light source and monomer solution (Fig 1). Polymerization occurs rapidly under transparent bands that nearly transmit the full light intensity from the source which results in raised ridges. Reflected light within the sample and migration of reactive chains cause slow polymerization in areas under the reflective bands and generate grooves between ridges. As a result, a pattern of parallel micro-ridges and grooves of uniform width and amplitude rapidly develop across the entire substrate surface in a single fabrication step (Fig 1). As expected, each ridge and groove was approximately 25 μm wide. Smooth transitions between the ridges and grooves were observed in place of sharp features generated by other photolithographic methods. Typical sample amplitude, from the highest point on ridges to the lowest point in adjacent grooves, ranged from 0.6 to 1.8 μm depending on polymerization conditions (Fig 3).

NIH-PA Author Manuscript

NIH-PA Author Manuscript

NIH-PA Author Manuscript

3.3. Micropatterned MA polymers direct dissociated SGN neurite growth *in vitro*

Having demonstrated the ability of MA polymers to support SG cell growth and survival, we next examined the influence of micropatterning on *de novo* neurite growth. Dissociated spiral ganglion cultures were plated on patterned or unpatterned 40%HMA/60%HDDMA polymers and maintained in BDNF and NT-3 for two days. In these experiments, the ridge periodicity was 50 μm and the channels were between 0.6 and 1 μm deep. Fixed cultures were immunostained with anti-NF200 antibody and digital epifluorescence images were captured. Dissociated SGN neurites wandered randomly on unpatterned HMA/HDDMA (Fig. 4A), similar to neurites on laminin coated slides (Roehm et al., 2008). By contrast, dissociated SGN neurites closely aligned with micropatterned HMA/HDDMA (Fig. 4B). To evaluate the extent of alignment to the pattern, we compared the ratio of the overall neurite length with the end-to-end distance of a straight line drawn from the cell body to the neurite terminus in parallel with the micropattern. A ratio of neurite length to end-to-end distance with values close to unity implies that the neurite closely follows the pattern whereas a ratio significantly greater than one implies that the neurite deviates from the pattern. The ratio of neurite length to end-to-end distance was 1.20±0.32 (mean±SD) on patterned HMA/HDDMA and 2.64±2.34 (mean±SD) on unpatterned HMA/HDDMA ($p<0.001$, Student's unpaired two tailed t-test). Thus, neurites on unpatterned HMA/HDDMA tend to grow in random directions reflected by the increased mean ratio of neurite length to end-to-end distance and the larger standard deviation. By contrast, nearly all neurites on patterned polymer closely align with the pattern. Thus, micropatterns with channel depth between 0.6 and 1 μm strongly direct dissociated SGN neurite growth *in vitro*.

3.4. Micropatterns induce spiral ganglion Schwann cell alignment in the absence of neurites *in vitro*

We noted close alignment of SGSCs with SGN neurites and with the pattern. Since growing SGN neurites closely align with SCs (Bostrom et al.,; Whitlon et al., 2009), it was difficult to determine whether the SC alignment was due to the influence of the pattern and/or the neurites. Thus, we next sought to determine the extent to which micropatterned MA polymers influence the alignment of SGSCs in the absence of neurites. Dissociated SG cultures were maintained in the absence of neurotrophic factors. In these conditions, over 90% of the neurons die (Hansen et al., 2001a; Hegarty et al., 1997). Cultures were immunostained with anti-S100 antibody to identify SCs and anti-NF200 antibody to verify lack of SGN processes in the vicinity. Fibroblasts were identified based on typical broad based stellate morphology and lack of S100-immunoreactivity. Subsets of cultures were immunostained with anti-vimentin antibodies to verify the fibroblastic morphology. Cell orientation was determined by drawing the outline of the cell using Image J software and fitting an ellipse to the cell outline. The angle of the long axis of the ellipse relative to the pattern (θ) was then measured in Image J (Fig. 5). The mean ellipse angle was 42.1±24.1 (mean±SD) for SCs on unpatterned HMA/HDDMA, 40.4±26.9 (mean±SD) for fibroblasts on patterned HMA/HDDMA, and 20.3±19.9 (mean±SD) for SCs on patterned HMA/HDDMA ($p<0.001$, ANOVA with post-hoc Dunn's Method revealing significant difference between orientation of SCs on patterned polymer with that of SCs on unpatterned polymer as well as fibroblasts on patterned polymer). We considered cells with an ellipse angle less than 10 to be aligned with the pattern. On unpatterned HMA/HDDMA, only 11.3% of the SCs aligned to the horizontal whereas 41.5% of SCs on patterned HMA/HDDMA were aligned to the pattern (Fig. 5). Fibroblasts failed to align with patterned HMA/HDDMA. Thus, SCs and fibroblast behave differently on the micropatterned HMA/HDDMA polymers used here implying that the ability of these micropatterns to induce cell alignment depends on cell-type.

NIH-PA Author Manuscript

NIH-PA Author Manuscript

NIH-PA Author Manuscript

3.5. Spiral ganglion Schwann cells remained aligned to SGN neurites *in vitro*

Although most SGN neurites and SGSCs remain closely aligned with the micropatterns, there are occasional primary neurites or branches that fail to parallel the pattern. We asked whether the SCs associated with these wandering neurites would parallel the pattern or whether they would align themselves with the neurites. In cultures immunolabeled with anti-NF200 and anti-S100 antibodies, we examined the relationship between neurite and SC when neurites do not follow the micropattern. In each case, the SCs associated with the neurites remained aligned to the direction of the neurite rather than the pattern (Fig. 6).

3.6. Micropatterns induce turning of neurites from spiral ganglion explants *in vitro*

Above we demonstrated that MA micropatterns strongly promote alignment of *de novo* neurite growth from dissociated SGNs. To determine whether the micropattern could induce turning of an already exiting neurite we used SG explants. These were placed in a central area lacking patterned polymer allowing the neurites to extend out from the explant until they encountered the pattern. Control explants were grown on unpatterned polymers or laminin-coated glass. As shown in Fig. 7, HMA/HDDMA polymers supported robust neurite outgrowth. Neurites extend radially from explants initially until encountering the micropattern which induces neurites to turn parallel to the pattern. Together with the neurites, SGSCs extended several hundred microns from the explant, however, S100-negative cell outgrowth was restricted, traveling only a fraction of the distance from the explant when compared to S100-positive SGSCs and their associated neurites (Fig. 7).

To quantify the influence of the pattern on SGN neurite growth, we measured the angle of neurites relative to the pattern as described in the methods section. On glass (n=69 neurites) and unpatterned polymers (n=150), neurites extended radially with no consistent directional turning, whereas neurites on patterned polymers (n=108) consistently turned to parallel the pattern.

Scatterplots of the angle of the initial neurite segment relative to the pattern compared with the difference between the initial and terminal angle relative to the pattern ($\Delta\theta$) illustrate the influence of the pattern on neurite growth (Fig. 8). If neurites grow radially and do not turn relative to the pattern, the $\Delta\theta$ is low and does not correlate with the initial angle to the pattern. Turning of a neurite to parallel the pattern results in strong correlation of the $\Delta\theta$ with the initial angle. As shown in the scatterplots (Fig. 8), the extent of neurite turning ($\Delta\theta$) strongly correlates with the initial angle on patterned polymer ($r=0.89$, $p<0.001$), but not on unpatterned polymer or glass ($r=0.05$, $p=0.56$ and $r=0.20$, $p=0.1$, respectively). Thus, on patterned polymers, the extent of neurite turning depends directly on the angle at which the neurite encounters the pattern. For example, neurites that encounter the pattern with a large initial angle (close to perpendicular) eventually turn to parallel the pattern as exhibited by their large degree of turning (Fig 8D). Therefore, on the described topographic features, final alignment of terminal neurite segments appears to be independent of their initial angle relative to the pattern. These results demonstrate that micropatterned methacrylate polymers strongly direct neurite growth and induce turning of established neurites independent of the original growth direction.

3.7. Neurites grow within the grooves of microchannels *in vitro*

To determine the location of neurites in the micropatterns, we used laser scanning confocal microscopy to create z-stacks of cultures grown on micropatterned MA polymers and immunostained with anti-NF200 and anti-S100 antibodies. Images were collected every 0.3μm beginning in the unpatterned area of the polymer and continuing through the thickness of the pattern (typically ~3 μm). In these stacks, it is easy to distinguish the ridges from the grooves since the ridges appear as acellular stripes lacking S100 immunoreactivity

NIH-PA Author Manuscript

NIH-PA Author Manuscript

NIH-PA Author Manuscript

whereas the grooves are the stripes that first appear in the stack with cellular labeling. As shown in Fig. 9, SGN neurites grew within the grooves of the micropatterned HMA/HDDMA polymers. The darker stripes running horizontally across Fig. 9 denote acellular regions, which represent ridges. The NF200 positive neurite remained in the cell-filled groove between ridges. This point is also illustrated in a stack of images rotated to view down the x-axis through the depth of the channels (Fig. 9). The NF200 positive neurite (red) remained in the groove.

4. Discussion

Significant further advances in cochlear implant technology will likely require tissue-engineering approaches to enhance the neural prosthesis interface (Pettingill et al., 2007). Use of defined substrate patterns has recently emerged as a potential tool to precisely control patterns of neural growth and circuitry. Here we leveraged the biocompatibility of MA polymers coupled with our ability to induce stable microchannels by photopolymerization to begin to explore the response of SGNs and SGSCs to specific topographical features. Our results demonstrate the ability of SG explants and dissociated cultures to survive and grow on various polymethacrylate substrates both with and without laminin extracellular matrix coating. These results are consistent with the well-established biocompatibility of MA polymer systems. Further, our data indicate that SGNs tolerate changes in the monomer proportions without substantial impact on survival or neurite outgrowth. This broad biocompatibility with neural cells may prove advantageous in future application by allowing engineers to maximize the physical characteristics of a potential polymer without compromising the tissue interface (Brors et al., 2002).

In addition to biocompatibility, MAs are useful for cellular studies that require control of spatial features since they readily undergo photopolymerization in the presence of a photoinitiator (Bryant et al., 2007). The spatial and temporal control afforded by photopolymerization, in addition to its mild reaction conditions make it a facile fabrication method to generate designed microtopographic features for the study of cellular response and alignment to patterned polymer substrates. Furthermore, process parameters such as light intensity and photoinitiator concentration of this single fabrication step can be modified to create a range of channel widths, depths, and curvatures that may be tailored to elicit varied cellular responses. For example, the width of the parallel micro-ridges and grooves can be modulated by varying the periodicity or band spacing of the photomasks. Moreover, topographic features such as total ridge amplitude and ridge-groove curvature can be manipulated by the temporal control enabled by photopolymerization in the form of total light dosage to the substrate or duration of light application. This spatial and temporal control will allow future investigations to develop and characterize critical topographic features that guide SGN neurite growth and SC alignment in order to improve the neural interface.

Enhancement of the CI prosthesis neural interface will likely require regrowth of peripheral SGN axons towards a stimulating electrode in an organized, radial pattern reflecting the normal afferent cochlear innervation (Pettingill et al., 2007; Roehm et al., 2005). Our results demonstrate a strong influence on SGN neurite guidance provided by micropatterns. Previous studies found that laminin patterned stripes result in SC alignment and hence enhanced neurite regeneration (Branch et al., 2001; Branch et al., 1998; Gustavsson et al., 2007; Miller et al., 2001; Oliva et al., 2003; Schmalenberg et al., 2005). Consistent with our results, topographical microfeatures generated by physical stamps (e.g. PDMS) promote alignment of PC12 cell processes (Foley et al., 2005). Further, a combination of microgrooves and laminin coating in the grooves acted synergistically to direct dorsal root ganglion neurite growth (Foley et al., 2005; Miller et al., 2001). Thus, impregnatation of

NIH-PA Author Manuscript

NIH-PA Author Manuscript

NIH-PA Author Manuscript

micropatterned methacrylate polymers with one or more species of bioactive molecules may further enhance SG neurite regeneration and provide additional directional cues.

In contrast to the sharply defined microfeatures generated by physical stamps, the photopolymers used here provide unique gradually sloped, shallow channeled characteristics that nevertheless induced SGSC alignment and SG neurite guidance in both explants and dissociated cultures. Further studies shall elicit the manner and order in which they align. The SG neurite growth cone could be influenced by the subtle topographical changes in the center of the channel, or it could respond to the channel walls, inducing a directional change back to the center of the trough as the neurite meanders within the confines of the channel.

Alternative strategies to guide neurite regeneration include the use of soluble factors (Richardson et al., 2009; Wise et al., 2005; Wise et al., 2010; Wittig et al., 2005). These present potential hurdles in the context of CIs, such as maintaining a precise concentration gradient of bioactive molecules in the direction of the CI electrode and the need to maintain bioactivity and stability through the production process. The use of physical cues overcomes many of these potential limitations.

Regeneration of functional auditory nerve fibers will likely require appropriate myelination; significantly, we found that the same topographic features that direct SGN neurite growth also promote alignment of SGSCs in the absence of neurites suggesting that both neural and glial elements respond to similar microfeatures. Given the ability of SCs to promote and direct axon regeneration, this influence of the topography on SGSCs could certainly enhance the guidance cues for SG neurites provided by micropatterns as seen in previous studies (Hsu et al., 2007). In the case of dissociated SGN cultures, one could imagine the SGSCs adjacent to SGN cell bodies aligning with the pattern prior to SG neurite regeneration. This would result in experimental conditions seen in previous studies in which substrates covered with SCs aligned with laminin stripes directed neurite growth (Schmalenberg et al., 2005). The tendency of neurites and SCs to remain aligned to one another even when not conforming to the direction of the micropattern further highlights the significance of the mutual influence these cells exert on each other.

In contrast to SCs, we found that fibroblasts in the SG cultures did not align to the micropattern. The micropattern's directing effect on SGSCs and neurites but not on fibroblasts could translate into a clinical advantage. CI performance can be limited by fibrous encapsulation resulting in increased impedence and subsequent increased current requirements (Paasche et al., 2009; Tykocinski et al., 2005). Indeed, efforts are underway to manipulate current electrode designs to limit fibroblast growth and subsequent encapsulation (Paasche et al., 2009; Rebscher et al., 2008). We observed SGSCs and SG neurite growth outpacing fibroblasts across the polymer surface. Future *in vivo* experiments will reveal the impact of this effect on fibrous encapsulation.

These results demonstrate the overall compatibility of MA polymers with cells derived from the SG and the profound influence of topographic microfeatures to differentially direct growth of these cells. The versatility of photopolymerization to create a variety of specific topographies will allow future studies to identify those features most critical for axon guidance. Such features may ultimately prove helpful in improving the neural prosthesis interface in future CI technology.

Research Highlights

- Methacrylate polymers support spiral ganglion neuron survival and neurite growth, even in the absence of extracellular matrix proteins.

NIH-PA Author Manuscript

NIH-PA Author Manuscript

NIH-PA Author Manuscript

- Photopolymerization creates highly reproducible micropatterns in methacrylate polymers.
- Photo-induced micropatterns strongly direct SGN neurite growth and spiral ganglion Schwann cell, but not fibroblast, alignment.
- SGN neurites typically grow within the grooves of micropatterned methacrylate polymers.
- The use of micropatterned surfaces to direct axon regeneration may lead to improved spatial resolution provided by cochlear implants.

Supplementary Material

Refer to Web version on PubMed Central for supplementary material.

Acknowledgments

Support: This work was supported by Grant Number UL1RR024979 from the National Center for Research Resources (NCRR), a part of the National Institutes of Health (NIH) and a grant from the American Hearing Research Foundation (AHRF). Its contents are solely the responsibility of the authors and do not necessarily represent the official views of the CTSA, NIH, or AHRF.

References

Alam SA, Robinson BK, Huang J, Green SH. Prosurvival and proapoptotic intracellular signaling in rat spiral ganglion neurons in vivo after the loss of hair cells. The Journal of comparative neurology. 2007; 503:832–852. [PubMed: 17570507]

Altschuler RA, Cho Y, Ylikoski J, Pirvola U, Magal E, Miller JM. Rescue and regrowth of sensory nerves following deafferentation by neurotrophic factors. Annals of the New York Academy of Sciences. 1999; 884:305–311. [PubMed: 10842602]

Apple DJ, Sims J. Harold Ridley and the invention of the intraocular lens. Survey of ophthalmology. 1996; 40:279–292. [PubMed: 8658339]

Bostrom M, Khalifa S, Bostrom H, Liu W, Friberg U, Rask-Andersen H. Effects of neurotrophic factors on growth and glial cell alignment of cultured adult spiral ganglion cells. Audiology & neuro-otology. 2009; 15:175–186. [PubMed: 19851064]

Branch DW, Wheeler BC, Brewer GJ, Leckband DE. Long-term stability of grafted polyethylene glycol surfaces for use with microstamped substrates in neuronal cell culture. Biomaterials. 2001; 22:1035–1047. [PubMed: 11352085]

Branch DW, Corey JM, Weyhenmeyer JA, Brewer GJ, Wheeler BC. Microstamp patterns of biomolecules for high-resolution neuronal networks. Medical & biological engineering & computing. 1998; 36:135–141. [PubMed: 9614762]

Brors D, Bodmer D, Pak K, Aletsee C, Schafers M, Dazert S, Ryan AF. EphA4 provides repulsive signals to developing cochlear ganglion neurites mediated through ephrin-B2 and -B3. The Journal of comparative neurology. 2003; 462:90–100. [PubMed: 12761826]

Brors D, Aletsee C, Schwager K, Mlynski R, Hansen S, Schafers M, Ryan AF, Dazert S. Interaction of spiral ganglion neuron processes with alloplastic materials in vitro(1). Hearing research. 2002; 167:110–121. [PubMed: 12117535]

Bryant SJ, Cuy JL, Hauch KD, Ratner BD. Photo-patterning of porous hydrogels for tissue engineering. Biomaterials. 2007; 28:2978–2986. [PubMed: 17397918]

Bryant SJ, Chowdhury TT, Lee DA, Bader DL, Anseth KS. Crosslinking density influences chondrocyte metabolism in dynamically loaded photocrosslinked poly(ethylene glycol) hydrogels. Annals of biomedical engineering. 2004; 32:407–417. [PubMed: 15095815]

Clark P, Connolly P, Curtis AS, Dow JA, Wilkinson CD. Cell guidance by ultrafine topography in vitro. Journal of cell science. 1991; 99(Pt 1):73–77. [PubMed: 1757503]

NIH-PA Author Manuscript

NIH-PA Author Manuscript

NIH-PA Author Manuscript

Curtis A, Wilkinson C. Topographical control of cells. Biomaterials. 1997; 18:1573–1583. [PubMed: 9613804]

Dalby MJ, Riehle MO, Yarwood SJ, Wilkinson CD, Curtis AS. Nucleus alignment and cell signaling in fibroblasts: response to a micro-grooved topography. Experimental cell research. 2003; 284:274–282. [PubMed: 12651159]

Danneman PJ, Mandrell TD. Evaluation of five agents/methods for anesthesia of neonatal rats. Laboratory animal science. 1997; 47:386–395. [PubMed: 9306312]

Dazert S, Kim D, Luo L, Aletsee C, Garfunkel S, Maciag T, Baird A, Ryan AF. Focal delivery of fibroblast growth factor-1 by transfected cells induces spiral ganglion neurite targeting in vitro. J Cell Physiol. 1998; 177:123–129. [PubMed: 9731752]

Dunn GA, Brown AF. Alignment of fibroblasts on grooved surfaces described by a simple geometric transformation. Journal of cell science. 1986; 83:313–340. [PubMed: 3805145]

Evans AJ, Thompson BC, Wallace GG, Millard R, O'Leary SJ, Clark GM, Shepherd RK, Richardson RT. Promoting neurite outgrowth from spiral ganglion neuron explants using polypyrrole/BDNF-coated electrodes. Journal of biomedical materials research. 2009; 91:241–250. [PubMed: 18814235]

Evans AR, Euteneuer S, Chavez E, Mullen LM, Hui EE, Bhatia SN, Ryan AF. Laminin and fibronectin modulate inner ear spiral ganglion neurite outgrowth in an in vitro alternate choice assay. Developmental neurobiology. 2007

Foley JD, Grunwald EW, Nealey PF, Murphy CJ. Cooperative modulation of neuritogenesis by PC12 cells by topography and nerve growth factor. Biomaterials. 2005; 26:3639–3644. [PubMed: 15621254]

Fozdar DY, Lee JY, Schmidt CE, Chen S. Hippocampal neurons respond uniquely to topographies of various sizes and shapes. Biofabrication. 2 035005.

Gustavsson P, Johansson F, Kanje M, Wallman L, Linsmeier CE. Neurite guidance on protein micropatterns generated by a piezoelectric microdispenser. Biomaterials. 2007; 28:1141–1151. [PubMed: 17109955]

Hansen MR, Vijapurkar U, Koland JG, Green SH. Reciprocal signaling between spiral ganglion neurons and Schwann cells involves neuregulin and neurotrophins. Hearing research. 2001a; 161:87–98. [PubMed: 11744285]

Hansen MR, Zha XM, Bok J, Green SH. Multiple distinct signal pathways, including an autocrine neurotrophic mechanism, contribute to the survival-promoting effect of depolarization on spiral ganglion neurons in vitro. J Neurosci. 2001b; 21:2256–2267. [PubMed: 11264301]

Hegarty JL, Kay AR, Green SH. Trophic support of cultured spiral ganglion neurons by depolarization exceeds and is additive with that by neurotrophins or cAMP and requires elevation of [Ca2+]i within a set range. J Neurosci. 1997; 17:1959–1970. [PubMed: 9045725]

Hsu SH, Lu PS, Ni HC, Su CH. Fabrication and evaluation of microgrooved polymers as peripheral nerve conduits. Biomedical microdevices. 2007; 9:665–674. [PubMed: 17562182]

Hsu SH, Chen CY, Lu PS, Lai CS, Chen CJ. Oriented Schwann cell growth on microgrooved surfaces. Biotechnology and bioengineering. 2005; 92:579–588. [PubMed: 16261633]

Johansson F, Carlberg P, Danielsen N, Montelius L, Kanje M. Axonal outgrowth on nano-imprinted patterns. Biomaterials. 2006; 27:1251–1258. [PubMed: 16143385]

Kapoor Y, Thomas JC, Tan G, John VT, Chauhan A. Surfactant-laden soft contact lenses for extended delivery of ophthalmic drugs. Biomaterials. 2009; 30:867–878. [PubMed: 19010533]

Kenny SM, Buggy M. Bone cements and fillers: A review. Journal of Materials Science-Materials in Medicine. 2003; 14:923–938. [PubMed: 15348504]

Kim SH, Ha HJ, Ko YK, Yoon SJ, Rhee JM, Kim MS, Lee HB, Khang G. Correlation of proliferation, morphology and biological responses of fibroblasts on LDPE with different surface wettability. Journal of biomaterials science. 2007; 18:609–622.

Leake PA, Hradek GT. Cochlear pathology of long term neomycin induced deafness in cats. Hearing research. 1988; 33:11–33. [PubMed: 3372368]

Lee TY, Guymon CA, Jonsson ES, Hait S, Hoyle CE. Synthesis, initiation, and polymerization of photoinitiating monomers. Macromolecules. 2005; 38:7529–7531.

NIH-PA Author Manuscript

NIH-PA Author Manuscript

NIH-PA Author Manuscript

Miller C, Jeftinija S, Mallapragada S. Micropatterned Schwann cell-seeded biodegradable polymer substrates significantly enhance neurite alignment and outgrowth. Tissue engineering. 2001; 7:705–715. [PubMed: 11749728]

Miller JM, Le Prell CG, Prieskorn DM, Wys NL, Altschuler RA. Delayed neurotrophin treatment following deafness rescues spiral ganglion cells from death and promotes regrowth of auditory nerve peripheral processes: effects of brain-derived neurotrophic factor and fibroblast growth factor. J Neurosci Res. 2007; 85:1959–1969. [PubMed: 17492794]

Oliva AA Jr. James CD, Kingman CE, Craighead HG, Banker GA. Patterning axonal guidance molecules using a novel strategy for microcontact printing. Neurochemical research. 2003; 28:1639–1648. [PubMed: 14584818]

Paasche G, Tasche C, Stover T, Lesinski-Schiedat A, Lenarz T. The long-term effects of modified electrode surfaces and intracochlear corticosteroids on postoperative impedances in cochlear implant patients. Otol Neurotol. 2009; 30:592–598. [PubMed: 19546829]

Pameijer CH, Zmener O. Resin Materials for Root Canal Obturation. Dental Clinics of North America. 2010; 54:325–344. [PubMed: 20433981]

Pettingill LN, Richardson RT, Wise AK, O'Leary SJ, Shepherd RK. Neurotrophic factors and neural prostheses: potential clinical applications based upon findings in the auditory system. IEEE transactions on bio-medical engineering. 2007; 54:1138–1148. [PubMed: 17551571]

Phifer CB, Terry LM. Use of hypothermia for general anesthesia in preweanling rodents. Physiology & behavior. 1986; 38:887–890. [PubMed: 3823208]

Quick, DJ.; Anseth, KS. Gene Delivery in Tissue Engineering: A Photopolymer Platform to Coencapsulate Cells and Plasmid DNA, Pharmaceutical Research. Vol. Vol. 20. Netherlands: Springer; 2003. p. 1730-1737.

Ratner B, Hoffman A, Schoen F, Lemons J. An introduction to Materials in Medicine, 2nd edition. Biomaterials Science. 2004:10–11.

Rebscher SJ, Hetherington A, Bonham B, Wardrop P, Whinney D, Leake PA. Considerations for design of future cochlear implant electrode arrays: electrode array stiffness, size, and depth of insertion. J Rehabil Res Dev. 2008; 45:731–747. [PubMed: 18816423]

Richardson RT, Wise AK, Thompson BC, Flynn BO, Atkinson PJ, Fretwell NJ, Fallon JB, Wallace GG, Shepherd RK, Clark GM, O'Leary SJ. Polypyrrole-coated electrodes for the delivery of charge and neurotrophins to cochlear neurons. Biomaterials. 2009; 30:2614–2624. [PubMed: 19178943]

Ridley N. Intraocular acrylic lenses. Trans Ophthalmol Soc UK Oxford Ophthalmol Congr. 1951:617–621.

Roehm PC, Hansen MR. Strategies to preserve or regenerate spiral ganglion neurons. Current opinion in otolaryngology & head and neck surgery. 2005; 13:294–300. [PubMed: 16160524]

Roehm PC, Xu N, Woodson EA, Green SH, Hansen MR. Membrane depolarization inhibits spiral ganglion neurite growth via activation of multiple types of voltage sensitive calcium channels and calpain. Molecular and cellular neurosciences. 2008; 37:376–387. [PubMed: 18055215]

Rubinstein JT. How cochlear implants encode speech. Current opinion in otolaryngology & head and neck surgery. 2004; 12:444–448. [PubMed: 15377959]

Schmalenberg KE, Uhrich KE. Micropatterned polymer substrates control alignment of proliferating Schwann cells to direct neuronal regeneration. Biomaterials. 2005; 26:1423–1430. [PubMed: 15482830]

Shannon RV, Fu QJ, Galvin J 3rd. The number of spectral channels required for speech recognition depends on the difficulty of the listening situation. Acta Otolaryngol Suppl. 2004:50–54. [PubMed: 15219048]

Song M, Uhrich KE. Optimal micropattern dimensions enhance neurite outgrowth rates, lengths, and orientations. Annals of biomedical engineering. 2007; 35:1812–1820. [PubMed: 17616821]

Spoendlin H. Retrograde degeneration of the cochlear nerve. Acta otolaryngologica. 1975; 79:266–275.

Tykocinski M, Cohen LT, Cowan RS. Measurement and analysis of access resistance and polarization impedance in cochlear implant recipients. Otol Neurotol. 2005; 26:948–956. [PubMed: 16151342]

NIH-PA Author Manuscript

NIH-PA Author Manuscript

NIH-PA Author Manuscript

Uludag H, De Vos P, Tresco PA. Technology of mammalian cell encapsulation. Cells as Drug Delivery Platforms. 2000; 42:29–64.

Whitlon DS, Tieu D, Grover M, Reilly B, Coulson MT. Spontaneous association of glial cells with regrowing neurites in mixed cultures of dissociated spiral ganglia. Neuroscience. 2009; 161:227–235. [PubMed: 19324078]

Wise AK, Richardson R, Hardman J, Clark G, O'Leary S. Resprouting and survival of guinea pig cochlear neurons in response to the administration of the neurotrophins brain-derived neurotrophic factor and neurotrophin-3. The Journal of comparative neurology. 2005; 487:147–165. [PubMed: 15880560]

Wise AK, Hume CR, Flynn BO, Jeelall YS, Suhr CL, Sgro BE, O'Leary SJ, Shepherd RK, Richardson RT. Effects of localized neurotrophin gene expression on spiral ganglion neuron resprouting in the deafened cochlea. Mol Ther. 2010; 18:1111–1122. [PubMed: 20216530]

Wittig JH Jr. Ryan AF, Asbeck PM. A reusable microfluidic plate with alternate-choice architecture for assessing growth preference in tissue culture. J Neurosci Methods. 2005; 144:79–89. [PubMed: 15848242]

NIH-PA Author Manuscript
NIH-PA Author Manuscript
NIH-PA Author Manuscript

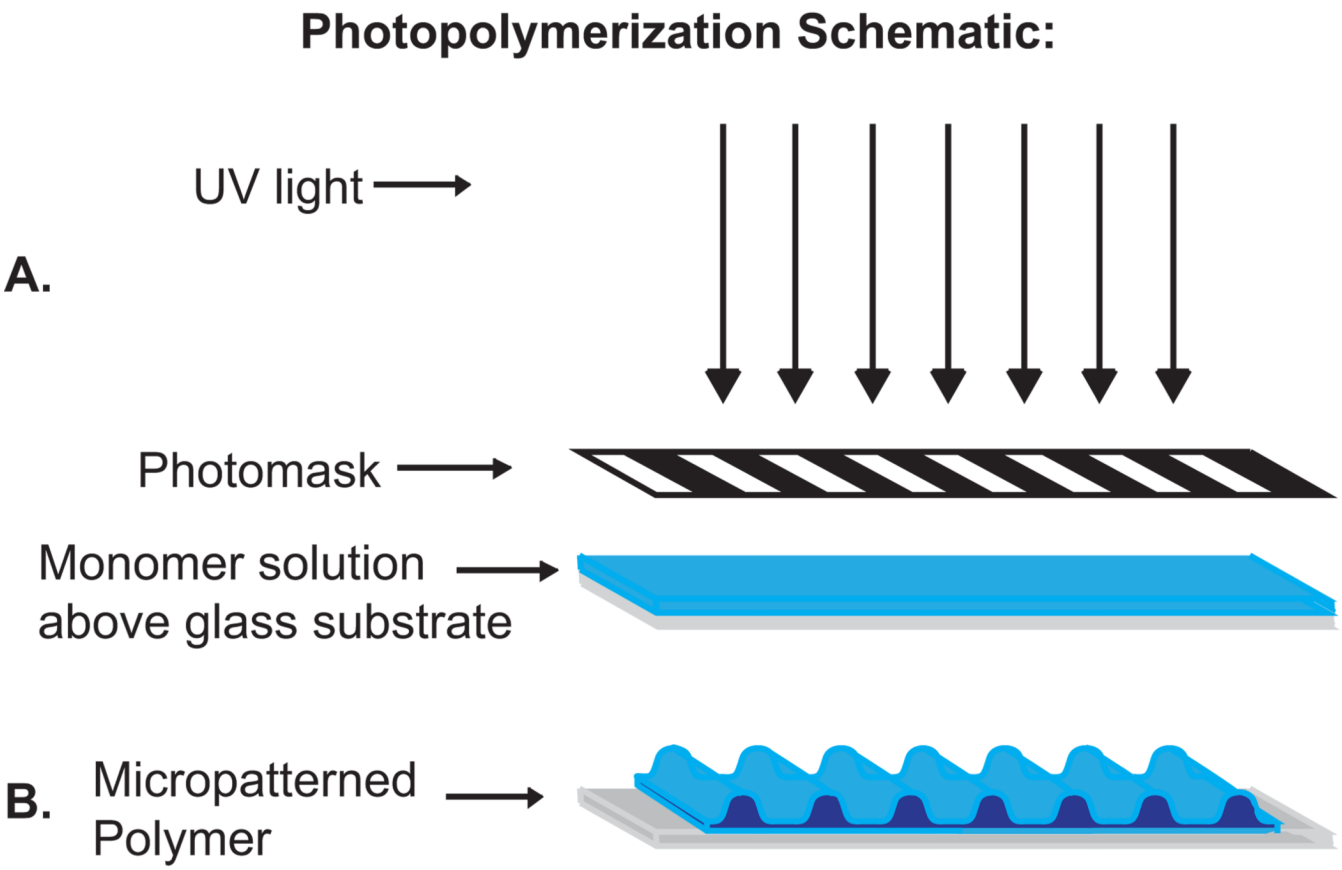

Figure 1.
Schematic of a photopatterning process. (A) Monomer solution is spread over a glass substrate. UV light passes through the mask photoinitiating the system. (B) Monomer that is exposed to UV polymerizes quickly and forms ridges while monomer in shadowed regions polymerizes slowly to form grooves between ridges.

NIH-PA Author Manuscript
NIH-PA Author Manuscript
NIH-PA Author Manuscript

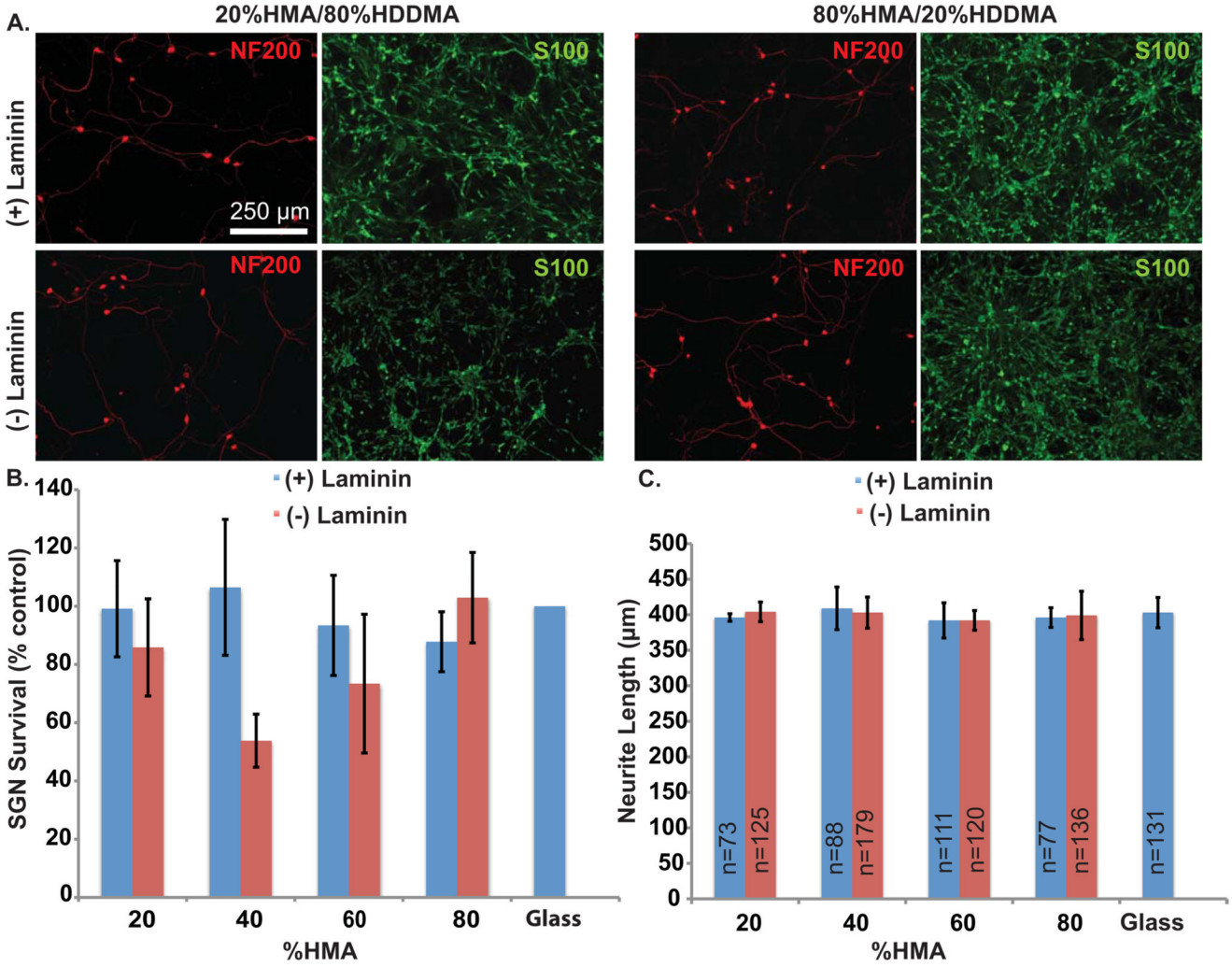

Figure 2.

SGN survival and neurite growth on HMA/HDDMA unpatterned polymer with and without laminin. (A) Dissociated SG cultures grown on 20%HMA/80%HDDMA (left) and 80%HDDMA/20%HMA (right) and immunostained with anti-NF200 (red) and anti-S100 (green) antibodies. Scale bar=250 µm. The top row represents cultures on laminin-coated polymer and the bottom row represents cultures on polymers without laminin coating. (B) SGN survival on indicated MA polymer composition with or without laminin coating. Legend indicates percent of HMA in HMA/HDDMA mixture. Neurons were cultured in three cloning cylinders for each condition with laminin coated glass used as control. Experiments were repeated in triplicate and survival was determined relative to control for each set of cultures. The average number of viable neurons counted across all controls was 521 +/− 258 (mean+/− SD) per well. There was no statistically significance difference in neurite survival among the different conditions (p=0.306, one way ANOVA). (C) SGN neurite length on indicated MA polymer composition with or without laminin coating. Legend indicates percent of HMA in HMA/HDDMA mixture and “n” represents the number of neurites measured in each condition. There was no statistically significance difference in neurite length among the different conditions (p=0.608, one way ANOVA)

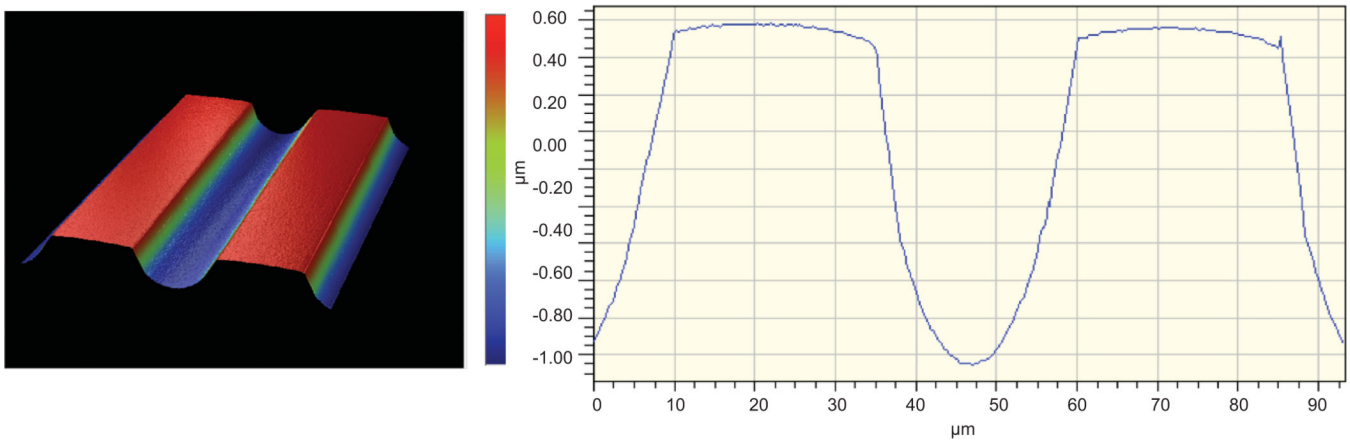

Figure 3.
Examples of a multicolor 3D (left) and graphical (right) schematic derived by interferometry characterizing photopolymerized microridges in methacrylate polymers with channel depth of ~1.8 µm.

NIH-PA Author Manuscript
NIH-PA Author Manuscript
NIH-PA Author Manuscript

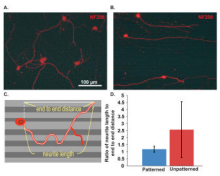

Figure 4.
Dissociated SGN neurite growth on unpatterned or patterned HMA/HDDMA. (A&B) Dissociated SG cultures grown on unnpatterned or patterned HMA/HDDMA and immunostained with anti-NF200 antibody. Neurite growth on unpatterned polymer is random whereas neurites on micropatterned polymers parallel the pattern. (C) Drawing represents measurement of neurite length as well as the measurement of cell body to nerve terminus parallel to the pattern used to assess the extent of neurite alignment to pattern. (D) Mean (+/− SD) ratios of neurite length to end-to-end distance for neurites on unpatterned or patterned HMA/HDDMA are significantly different by Student's unpaired two-tailed t-test ($p<0.001$).

NIH-PA Author Manuscript NIH-PA Author Manuscript NIH-PA Author Manuscript

NIH-PA Author Manuscript

NIH-PA Author Manuscript

NIH-PA Author Manuscript

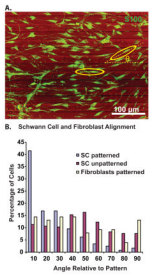

Figure 5.

Spiral ganglion Schwann cells, but not fibroblasts, align with micropatterns in the absence of neurites. (A) Cell alignment was determined by measuring the angle (θ) of an ellipse fitted to the major axis of the cell relative to the pattern. (B) Histogram of orientation angle for SCs and fibroblasts on patterned or unpatterned polymers (n=354, 300 and 76 for SC on patterned polymer, SC on unpatterned polymer and fibroblasts on patterned polymer respectively). Over 75% of SCs on patterned polymer were oriented within 30 degrees to the pattern. The difference in alignment of SCs on patterned polymers vs SC's on unpatterned polymers and fibroblasts on patterned polymers was significant ($p<0.001$, ANOVA with post-hoc Dunn's Method).

NIH-PA Author Manuscript
NIH-PA Author Manuscript
NIH-PA Author Manuscript

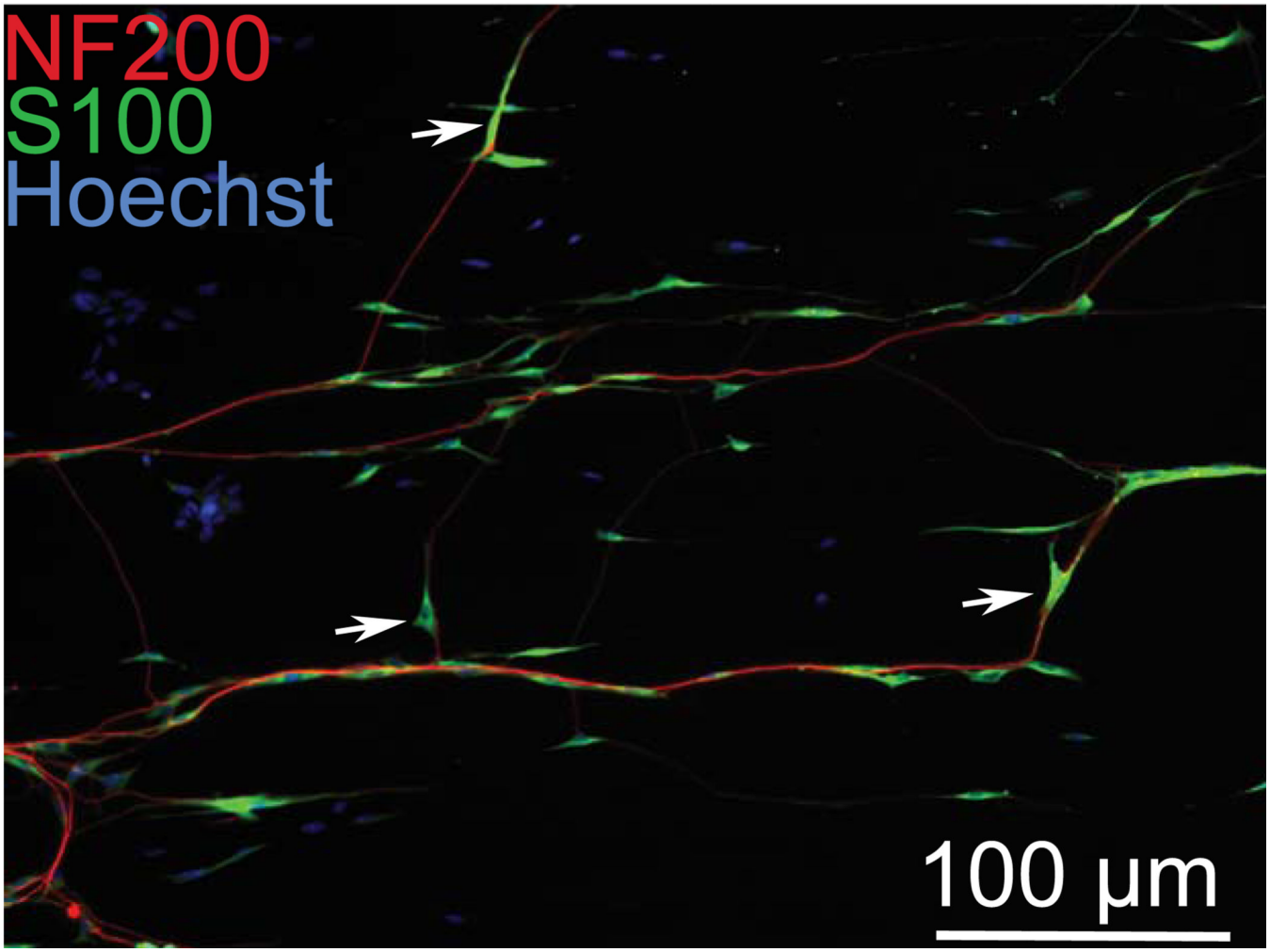

Figure 6.
Spiral ganglion Schwann cells remain closely associated with neurites even when they are not in line with the pattern. Dissociated SG culture on patterned HMA/HDDMA and immunostained with anti-NF200 (red) and anti-S100 (green) antibodies. Arrows denote SCs aligned with neurites that fail to follow the pattern, which is parallel to the horizontal plane.

NIH-PA Author Manuscript
NIH-PA Author Manuscript
NIH-PA Author Manuscript

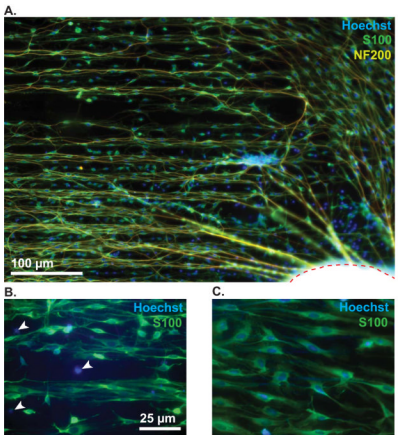

Figure 7.

Spiral ganglion explant on patterned HMA/HDDMA polymer. (A) The explant body is outlined with a dashed red line on the bottom right corner. NF200-labeled neurites (yellow) extend initially from the explant in a radial fashion and are subsequently induced to turn parallel to the pattern which is oriented along the horizontal plane. Anti-S100 antibody (green) and Hoechst (blue) were used to label SCs and nuclei respectively. Notably, there are several S100-negative cell nuclei clustered close to the explant, as exemplified in the higher magnification images below. (B) White arrowheads indicate S100-negative cell nuclei. (C) Image taken further away from the explant (~ 200 μm) demonstrating that all nuclei are associated with S100-positive cells. The micropatterned MAs support SC outgrowth more favorably than S100-negative cells such as fibroblasts.

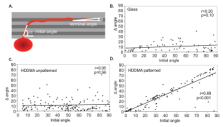

Figure 8.

Micropatterned HDDMA induced turning of SGN neurites from SG explants. (A) The initial neurite angle relative to the pattern was compared to the angle change from initial to terminal segment (Δθ) to determine the extent of turning by neurites in patterned and unpatterned polymer environments. (B–D) Scatterplots of SGN neurite growth on glass (B), unpatterned HDDMA (C) and HDDMA with micropaterning (D) demonstrate that neurite growth on micropatterned HDDMA has a direct correlation between the initial angle to the pattern and the angle change between the initial and terminal neurite segment.

NIH-PA Author Manuscript NIH-PA Author Manuscript NIH-PA Author Manuscript

NIH-PA Author Manuscript
NIH-PA Author Manuscript
NIH-PA Author Manuscript

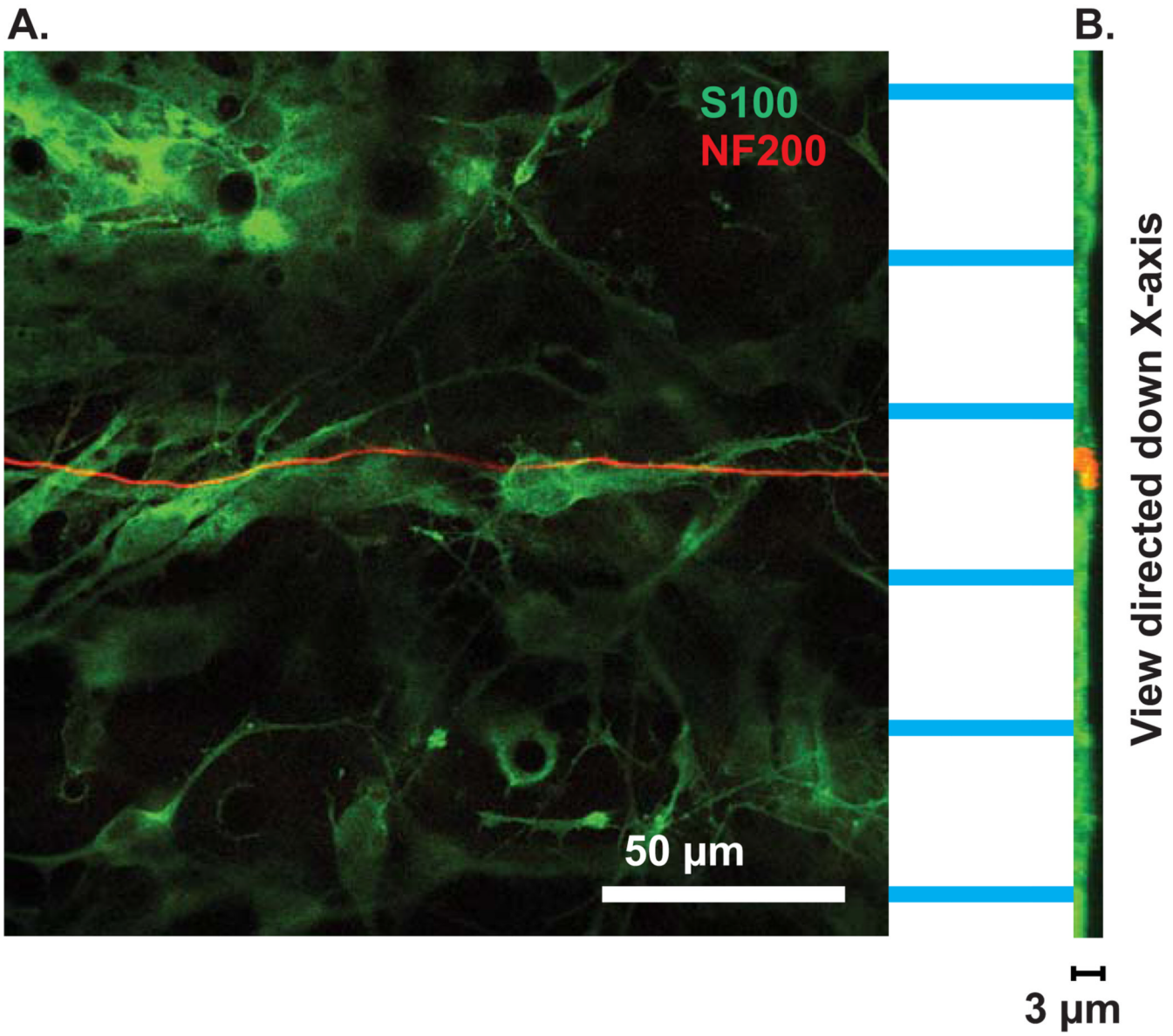

Figure 9.
SGN neurite grow within the microgrooves of patterned HMA/HDDMA. (A) Section of confocal z-stack from SG culture immunostained with anti-S100 (green) and anti-NF200 (red) antibodies. The neurite grows within the groove, demonstrated as a cellular stripe between acellular ridges. Scale bar=50 µm. (B) Ninety degree rotation of the stack to allow viewing down the x-axis. The grooves are evident as the regions with thicker S100 labeling compared with the ridges. The neurite (red) remains confined to the groove region. Scale bar=3 µm.